



Contents lists available at ScienceDirect

International Journal of Rock Mechanics & Mining Sciences

journal homepage: www.elsevier.com/locate/ijrmms

Technical Note

Using terrestrial 3D laser scanning and optical methods to determine orientations of discontinuities at a granite quarry

Ahmet Hamdi Deliormanli ^{a,b,*}, Norbert H. Maerz ^a, James Otoo ^a^a Missouri University of Science and Technology, Geological Engineering Department, USA^b Dokuz Eylul University, Mining Engineering Department, Turkey

ARTICLE INFO

Article history:

Received 30 January 2013

Received in revised form

17 August 2013

Accepted 24 December 2013

Available online 21 January 2014

1. Introduction

Joints are the most common rock discontinuities. They are generally considered as part of the rock mass. The spacing of joints is usually in the order of a few to tens of centimeters. Joints are constant features of the rock mass. Rock mass behavior is largely governed by joints. The role of rock joints in rock mass behavior includes: dividing rock into slabs, blocks and wedges; acting as planes of weakness for sliding and moving; providing channel, for water flow and creating flow networks; and altering the in situ stress distribution and orientation.

The determination of joint features especially orientation, is very important in the dimensional stone industry because of the roles joints play in the behavior of a rock mass. These structural features control the block size and affect the dimension stone production technique.

Studies of the orientation of jointing as a means of block size assessment are frequently found in research papers [1–9]. In addition to this, there are other studies in regard to dimensional stones. Yavuz et al. [10] studied the geological parameters such as bedding, joints, schist interlayers and mica filled joints affecting marble production in the quarries along the southern flank of the Menderes Massif, in SW Turkey. Nikolayev et al. [11] defined model-based prediction of unfractured rock masses using numerical analysis to determine the distribution of individual shapes, and volumes of in-situ blocks. Prissang et al. [12] studied on the localization of undisturbed blocks in larger dimension stone rock masses. Sousa [13] presented a granite fracture index to check suitability of granite outcrops for quarrying. Carvalho et al. [14]

focused on decision criteria for the exploration of marble deposits of the Portuguese Estremoz Anticline. Sousa [15] evaluated the influence of joint characteristics on block size assessment and defined a more reliable fracturation index for purposes of dimension stone.

Several methods have been used to evaluate the jointing orientation of rock masses. The joint orientations can be and have been traditionally measured using manual compass and clinometer methods. These methods are well known however; in practice there are significant problems and objections to the application of the manual field survey methods. Although these tools are effective, there are many errors inherent in the use of these methods. There are disadvantages in the use of manual field survey methods. They are slow, tedious, cumbersome, and erroneous. Apart from these disadvantages, direct access to rock faces is also often difficult or impossible. Additionally, dense vegetation, slope deposits or fences may hamper the physical access. Higher parts of the slope are impossible to reach without rock climbing equipment or scaffolding. Furthermore, discontinuity properties often vary a great deal throughout the rock mass, even within a small volume. Thus, a large amount of data is required to accurately describe behavior of a discontinuous rock mass. The uses of imaging technologies are on the increase to help overcome the problems with the manual methods. Developments in image capturing and laser scanning technology have increased their use in determining discontinuity features. A main advantage of three-dimensional laser scanning is that it allows the very rapid generation of a very detailed and accurate three-dimensional geometric representation of exposed rock faces. The geometric representation is in the form of a very dense three-dimensional point dataset, a so-called “point cloud”. Several researchers have studied the use of the three-dimensional laser scanning technique to calculate facet orientation [16–28]. This technique is not sufficient to determine trace orientation. Therefore; the optical

* Corresponding author at: Dokuz Eylul University, Mining Engineering Dept., Izmir, Turkey. Tel.: +90 232 301 7520; Fax: +90 232 453 0868.

E-mail address: ahmet.deliormanli@deu.edu.tr (A.H. Deliormanli).

image method is used to calculate trace orientation combined with point cloud [29–31].

The main objective of this research is to estimate the orientations of discontinuities in the Red Granite Quarry using point clouds and optical images obtained with a three-dimensional terrestrial scanner. To calculate the orientation of facets, point cloud data were used. To estimate trace orientations, optical images acquired using the inbuilt optical camera of the scanner, were used. Results of the study are presented in this paper.

2. Geology of the study area

The study was conducted at the Missouri Red Granite quarry, located in Iron County, Missouri. The quarry is specifically located in Graniteville, at latitude and longitude of $37^{\circ}39'01''$ and $-90^{\circ}40'47''$ about 5 miles from Ironton; the county seat of Iron County. Graniteville is known to have the largest and most important granite quarries in the state. The area is dominated by igneous rocks, mainly granite and rhyolite known to be of pre-Cambrian to Cambrian age, and has undergone some tectonic activities in the past which has resulted in the presence of several faults. The quarry is the major source of the granite production in the Missouri State. Dimensions of producing granite blocks are 3.14 by 0.92 by 1.51 m from open pit mining. The production is a combination of blasting, flaming and slot and wedging. In study area there are four active pits. While one of them is used for producing aggregates, the others are used for producing dimensional stone. In this study joint orientation measurements are subject to two pits which are Open pit-1 and Open pit-2.

3. Methods

Discontinuities have two manifestations in rock cuts. These are “facets” and “traces” (Fig. 1). Facets are actual exposures of the discontinuity walls while traces are intersections of the discontinuity with the cut plane [26]. In this study, orientations of facets were estimated from LiDAR data, while those of traces were estimated using optical images. The methodology of the study is summarized in Fig. 2 as a flowchart.

3.1. Manual measurements

Orientations of facets and traces were measured manually with a Brunton compass in the field. Locations and measurements for

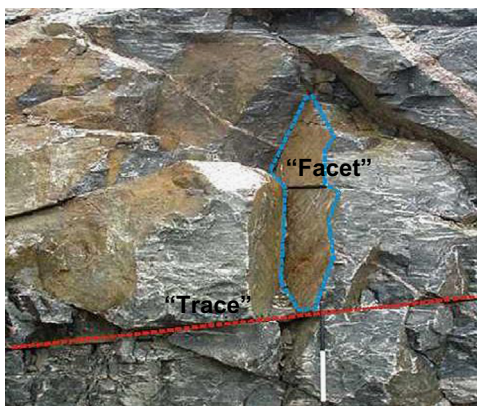


Fig. 1. Both fracture traces (red line) and facets (cyan polygon) [32]. (For interpretation of the references to color in this figure legend, the reader is referred to the web version of this article.)

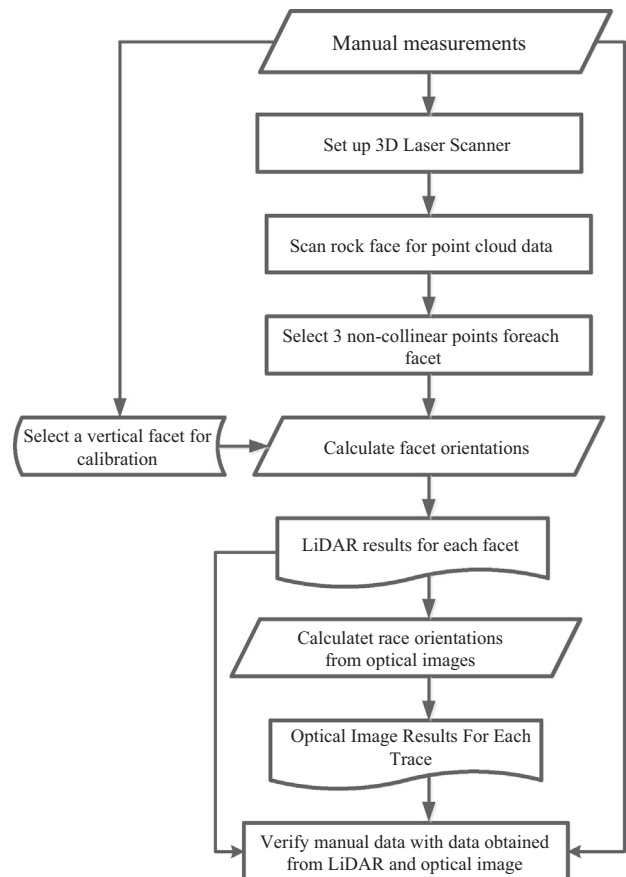


Fig. 2. Flow chart of the methodology of the study.

each joint were recorded in a survey notebook. Manual measurements were used not only for comparison but also for verification of the LiDAR and optical image measurements. A near vertical planar orientated facet measurement was used to reorient the point cloud data.

3.2. LiDAR Scans

LiDAR scans were obtained using a Leica ScanStation II scanner. The instrument has a dual window system that covers a $360 \times 270^{\circ}$ field of view. Scanning resolution of 4×4 mm was used in the point cloud data acquisition. Scanning distance is about 30 m for this resolution. Total scanning time at this resolution was about 20 min for each face of the quarry. Optical images were acquired before scanning, so that points in the point cloud can be colored with the optical color most closely associated with each scanned point. This enables the user to easily identify joint surfaces when browsing through the point cloud in the LiDAR viewer.

Cyclone software modules provide point cloud users with a wide set of work process options for 3D laser scanning in the study (Fig. 3). The software plays a critical role in handling and viewing high-definition point clouds effectively and aids in the speedy extraction of deliverables. A LiDAR point cloud is a set of points defined by x , y and z coordinates. The z (vertical) coordinates are inherently correct as the z -axis is always vertical, assuming the LiDAR scanner is correctly leveled. The x and y -axes can be arbitrarily oriented and represent the local coordinate system of the LiDAR scanner. Matching the LiDAR local coordinate systems to a global geographic coordinate system typically requires survey techniques that in addition to requiring additional personnel and surveying equipment increase the time required for measurements [33].

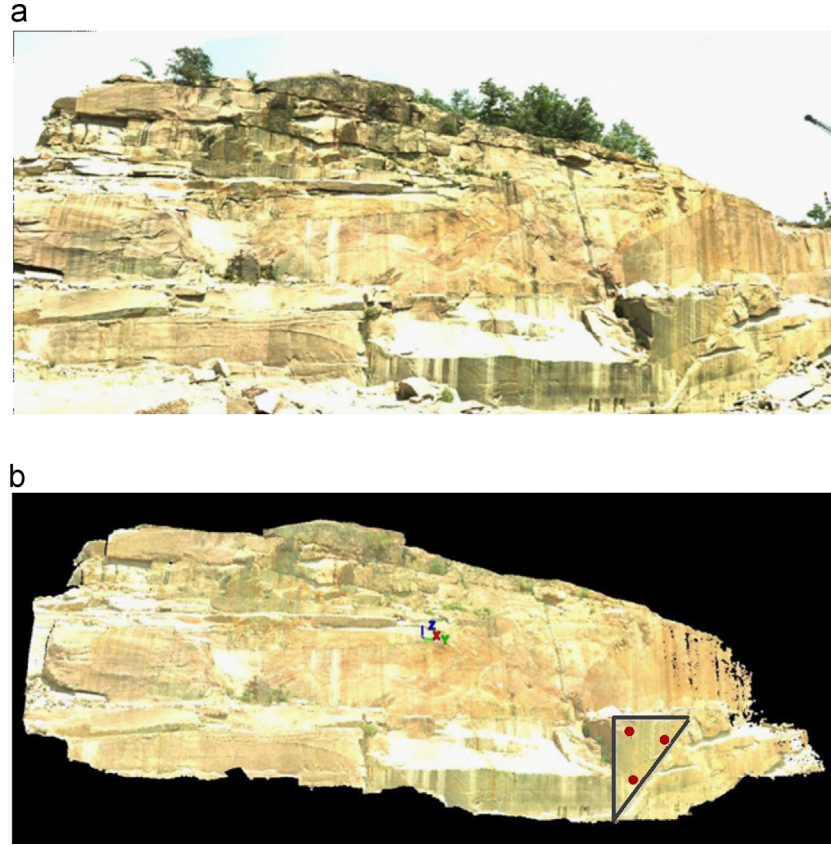


Fig. 3. Section of the Red Granite quarry. (a) Optical image generated by the LiDAR scanner (b) LiDAR scan (points overprinted with optical colors) and picking three points of a joint using a point cloud viewer in Cyclone software. (For interpretation of the references to color in this figure legend, the reader is referred to the web version of this article.)

For the first step of this method the discontinuity orientations are measured in the local coordinate system. During the second step discontinuity measurements are reoriented. A single sub-vertical discontinuity measurement called target plane is needed for the calibration of the measurements [33]. The true orientation of the target plane is obtained from the manual measurements. During the manual field measurements description and orientation of this plane is recorded clearly. The target plane may be different for each LiDAR setup.

Using the software viewer, three individual points on each facet to be measured are picked using the mouse cursor (Fig. 3(b)). These points should be spread out as far as possible on the same joint and care must be taken that the three points are not collinear or close to being collinear. The selected facet is numbered, and then the three data points are recorded in data sheet software for each facet. The dip and dip direction of the facet was then calculated using the three point program proposed in [33].

For the calculation of dip and dip direction, three co-planar points (but not co-linear) on a facet in a local coordinate space are selected by means of the software. Three points and the plane are defined as

$$P_1(x_1, y_1, z_1), \quad P_2(x_2, y_2, z_2), \quad P_3(x_3, y_3, z_3),$$

$$Ax + By + Cz + D = 0 \quad (1)$$

where (A, B, C) is the normal vector to the plane. The normal vector of the plane is calculated as

$$\mathbf{U} = (A, B, C) = \mathbf{P}_1\mathbf{P}_2 \times \mathbf{P}_1\mathbf{P}_3 = \begin{vmatrix} \mathbf{i} & \mathbf{j} & \mathbf{k} \\ x_2 - x_1 & y_2 - y_1 & z_2 - z_1 \\ x_3 - x_1 & y_3 - y_1 & z_3 - z_1 \end{vmatrix}$$

$$= [(y_2 - y_1)(z_3 - z_1) - (z_2 - z_1)(y_3 - y_1)]\mathbf{i} \\ - [(x_2 - x_1)(z_3 - z_1) - (z_2 - z_1)(x_3 - x_1)]\mathbf{j} \\ + [(x_2 - x_1)(y_3 - y_1) - (y_2 - y_1)(x_3 - x_1)]\mathbf{k} \quad (2)$$

The plane that passes through a point \mathbf{P}_1 and its normal vector is \mathbf{U} is calculated as follows:

$$\mathbf{U} \cdot \mathbf{P}_1\mathbf{P} = 0 \quad (3)$$

$$A(x - x_1) + B(y - y_1) + C(z - z_1) = 0 \quad (4)$$

$$Ax + By + Cz - Ax_1 - By_1 - Cz_1 = 0 \quad (5)$$

$$D = -Ax_1 - By_1 - Cz_1 \quad (6)$$

Note that “ D ” is not required for this calculation.

The normal vector of the plane is converted to unit normal vector as follows:

$$\mathbf{V} = \frac{\mathbf{U}}{\|\mathbf{U}\|} = \frac{1}{\sqrt{A^2 + B^2 + C^2}}(A, B, C) = (a, b, c) \quad (7)$$

The vector (a, b, c) is transformed into spherical coordinates (r, θ, φ) . Note that since we are concerned with unit normal on the unit hemisphere, r will always be equal to 1 so it will not be calculated.

$$a = r \sin \varphi \cos \theta \quad (8)$$

$$b = r \sin \varphi \sin \theta \quad (9)$$

$$c = r \cos \varphi \quad (10)$$

The values of φ and θ (in radians) are calculated as

$$\cos \varphi = c \quad (11)$$

$$\tan \theta = b/a \quad (12)$$

The value of φ is always between 0 and $\pi/2$ (0 and 90°) or between 0 and $-\pi/2$ (0 and -90°) while, the geographical coordinate system requires a value between 0 and 2π (0 and 360°) in a clockwise direction. Following this step, the φ angle is rotated from the local coordinate system to a global coordinate system. For this rotation process, data is obtained by manually measuring a single discontinuity in the field using a compass comparing the φ value measured in the field with the φ value calculated from the LiDAR data.

3.3. Measuring trend and plunge from an optical image

The trend and plunge of a trace on a rock cut will always be in the plane of the rock cut [34]. The following steps were taken in order to determine the trend and plunge from optical images.

Select any three non-collinear points on the rock facet and put these points in the three-point program to obtain the azimuth of the rock face. In cases where the rock face is not uniformly vertical as in Fig. 4, the azimuth should be determined for each face that has a trace.

Represent the azimuth with a two edged directional arrow, one edge to the left and the other edge to the right, with the azimuth clearly stated at each end.

Observe the inclination of the traces. Traces could be inclined to the left or to the right. Traces that inclined to the left of the image have trend values at the left end of the arrow, and traces that inclined to the right have trend values at the right end of the arrow.

Determine the acute angle between the trace and any horizontal line that crosses it. The acute angle between the trace and any horizontal line that crosses it is known as the rake. For vertical faces, this rake is always equal to the plunge of the trace. This plunge can be estimated using a protractor or by image processing algorithms.

4. Results and discussions

In this study, joint orientation measurements were carried out in two different regions. The region was named “Open pit-1”, and the other was named “Open pit-2”. Results of “Open pit-1” are



Fig. 4. LiDAR scan of a section of the Red Granite quarry face, showing facets labeled with digits in red ink and white background, and traces labeled with alphabets in blue ink. (For interpretation of the references to color in this figure legend, the reader is referred to the web version of this article.)

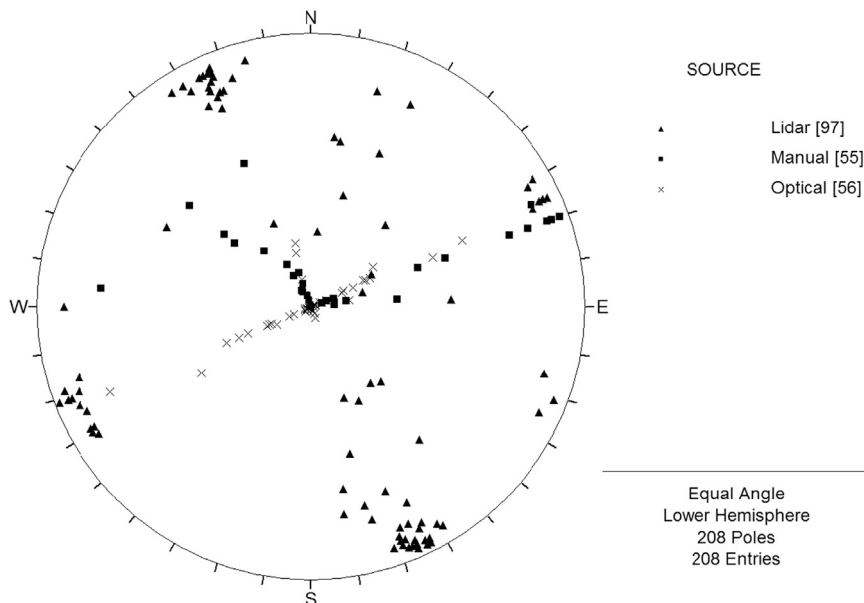


Fig. 5. Lower hemisphere projection for Open pit-1. (Red squares are manual measured discontinuities; blue triangles are LiDAR generated measurements, green circles are obtained from Optical-image). (For interpretation of the references to color in this figure legend, the reader is referred to the web version of this article.)

presented as a lower hemisphere stereographic projection plot in Fig. 5. Fifty-five manual measurements were made, while 153 LiDAR and optical image measurements were made. The lower hemisphere stereographic projection plot of the manually measured orientations in the Open pit-1 showed the presence of two dominant discontinuity sets; JS1-86/250 and JS2-2/245 (Fig. 6). One of these sets is nearly vertical and the other is almost horizontal. LiDAR and optical image results are presented as lower hemisphere stereographic projection plot in Fig. 7. The LiDAR and optical image results, show three dominant discontinuity sets, with average orientations of JS1-88/247, JS2-2/243 and JS3-87/156. Two sets are almost vertical while one is nearly horizontal. Discontinuity sets were tabulated to compare the two measurement methods (Table 1). The differences between the numbers of discontinuity sets are due to insufficient manual field measurements. This was because higher parts of the rock face which had a

high risk of rockfall, was avoided during the manual field measurements. However, the orientations of discontinuities in the higher areas of the rock face were easily measured from the LiDAR data. This result justifies the usefulness of both LiDAR and optical imaging techniques.

The measurement area for Open pit-2 was smaller than that of Open pit-1. Little difficulty was encountered during manual measurement in Open pit-2 when compared to Open pit-1. Measurement results are presented in Fig. 8. Eleven manual measurements were made. Twenty-nine LiDAR and optical measurements were obtained. Three dominant joint sets were observed from both the manual and LiDAR-optical measurements. Lower hemispherical stereographic projection plots of the manual and LiDAR-optical discontinuities measured in the Open pit-2 are presented in Figs. 9–10. The three dominant discontinuity sets have mean orientations of; JS1-84/237, JS2-4/46, and JS3-87/148 for manual field measurement and JS1-85/

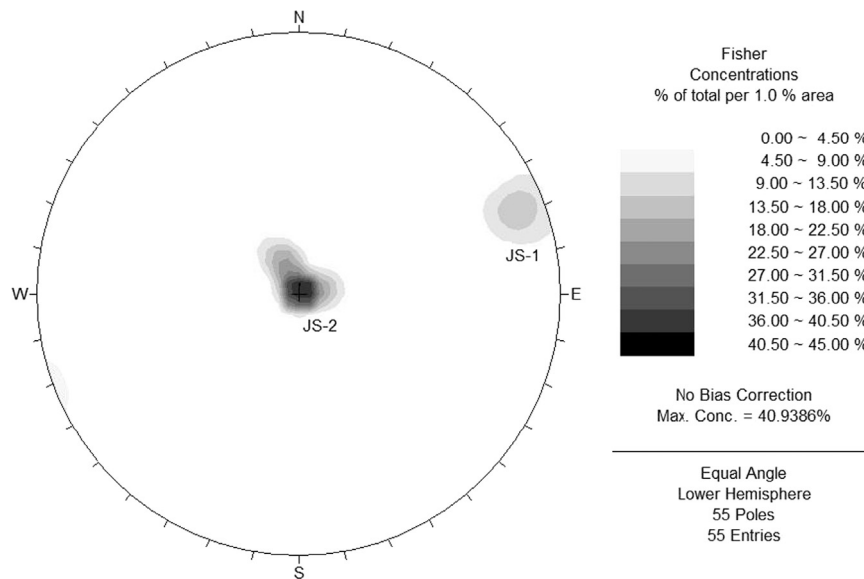


Fig. 6. Joint sets obtained from manual measurements for Open pit-1.

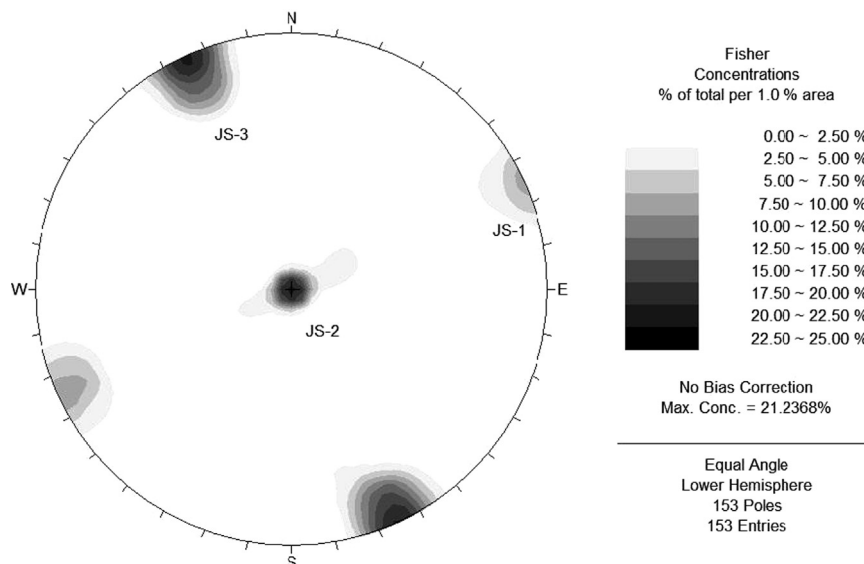


Fig. 7. Joint sets obtained from LiDAR and Optical image for Open pit-1.

231, JS2-4/45 and JS3-81/142 for LiDAR-optical field measurement. These results are summarized in Table 2. Two of the joint sets are nearly vertical, and one is sub-horizontal.

Results of manual and LiDAR-optical methods in both Open-pit 1 and Open pit 2 were very close. However, as shown in Open pit-1, difficulties in manual methods in field resulted in the lack of measurements at the upper area of the rock face. This is

a very important problem for engineering design projects, and again justifies, the fact that the LiDAR-optical method is more advantageous in determining discontinuity orientations than the manual method.

5. Conclusion

Joint orientation affecting block production and block size in the dimensional stone quarries is a significant primary geological parameter. For this reason, this parameter needs to be accurately determined. Identification of the joint orientation will contribute to the health development of dimensional stone quarry and also effective and economic use of the dimensional stone beds.

In the study two methods, a manual and a LiDAR-optical based were used to estimate joint orientations in the Red Granite Quarry located in Missouri, USA. Comparison of the joint orientation

Table 1
Summarized results of joint sets using both systems for Open pit-1.

Joint set	Manual		LiDAR-Optical	
	Dip	Dip direction	Dip	Dip direction
1	86	250	88	247
2	2	245	2	243
3			87	156

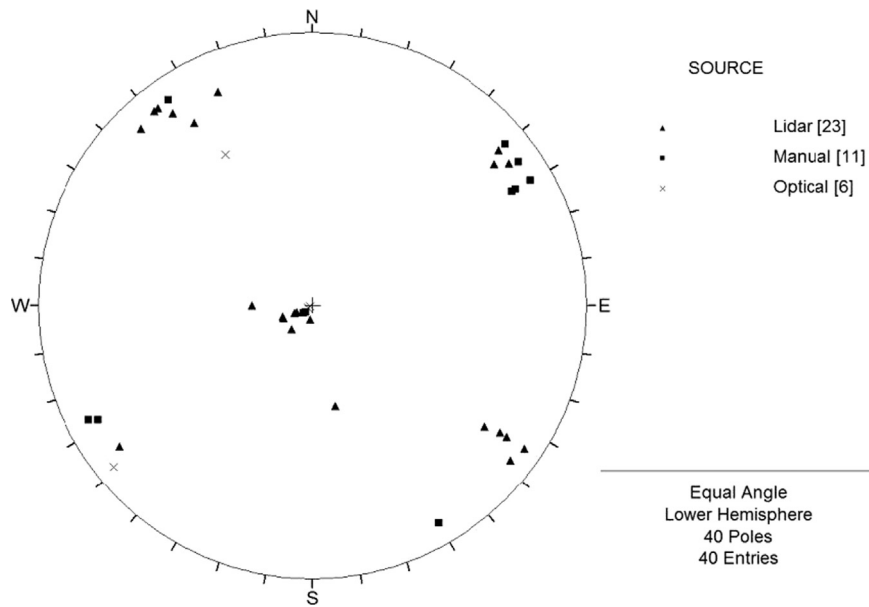


Fig. 8. Lower hemisphere projection for Open pit-2. (Red squares are manual measured discontinuities; blue triangles are LiDAR generated measurements, green circles are obtained from Optical-image.) (For interpretation of the references to color in this figure legend, the reader is referred to the web version of this article.)

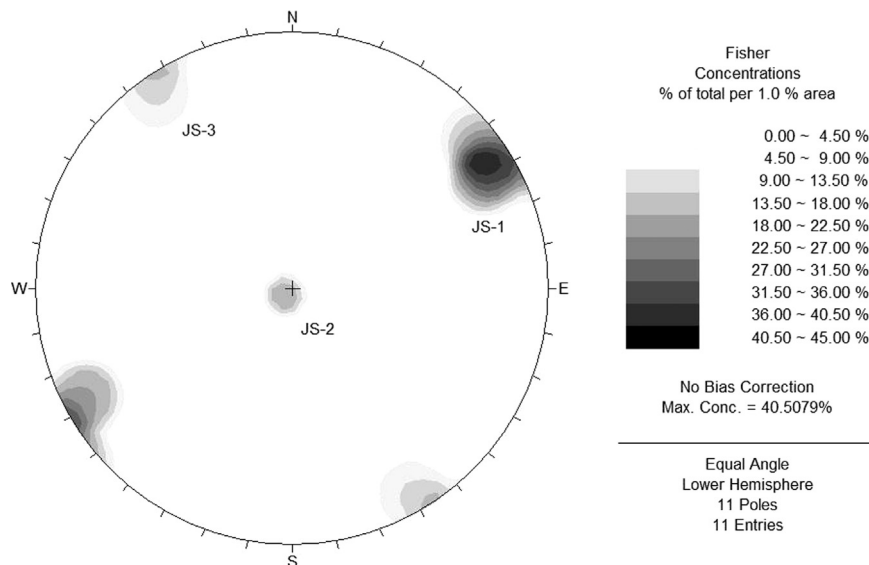


Fig. 9. Joint sets obtained from manual measurements for Open pit-2.

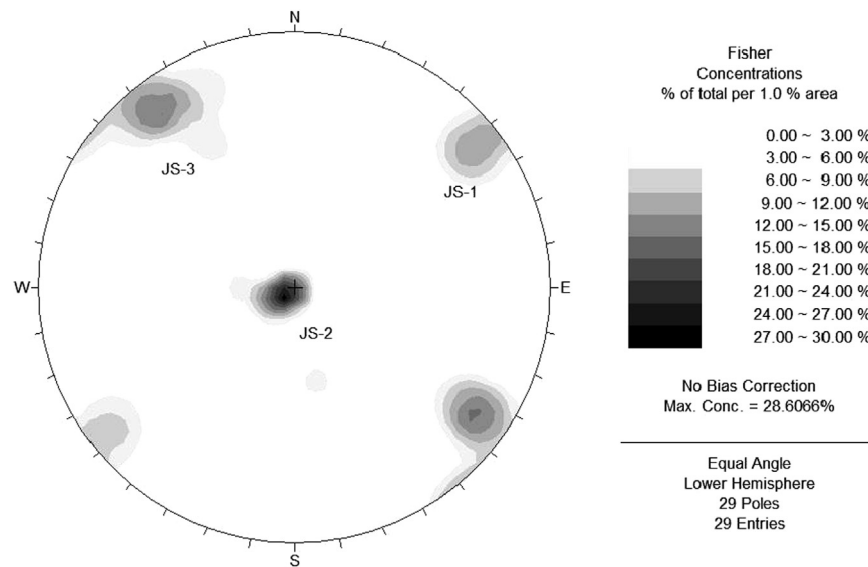


Fig. 10. Joint sets obtained from LiDAR and optical image for Open pit-2.

Table 2

Summarized results of joint sets using both systems for Open pit-2.

Joint set	Manual		LiDAR-Optical	
	Dip	Dip direction	Dip	Dip direction
1	87	237	85	231
2	4	46	4	45
3	87	148	81	142

results showed that the manually measured results are very close to the LiDAR-optical measurements. However, disadvantages of manual measurement, such as time consumption, bias sampling, and risk from falling rocks were encountered during manual measurements in Open pit-1 field.

Results of this study shows that the LiDAR-optical measurement method is more advantageous than manual (compass) measurement. Joint orientation data obtained from the LiDAR were quick and easy to collect, and also more accurate when compared to the manual method.

Acknowledgments

The authors would like to thank the National Science Foundation, and the Scientific and Technical Research Council of Turkey, (TUBITAK) for their financial support. Special thanks also go to the Red Granite Company, for providing their facility for this research.

References

- [1] Hudson JA, Priest JP. Discontinuities and rock mass geometry. *Int J Rock Mech Min Sci* 1979;16:339–62.
- [2] Toyos JM, Taboada J, Lombardero M, Romero JA, Menendez A. Estudio de las discontinuidades en yacimientos de roca ornamental. *Bol Geológico Min* 1994;105:110–8.
- [3] Lu P, Latham JP. Developments in the assessment of in-situ block size distributions of rock masses. *Rock Mech Rock Eng* 1999;30:29–49.
- [4] Palmström A. Measurement and characterization of rock mass jointing. In: Sharma VM, Saxena KR, editors. *In-situ Characterization of Rocks*. Rotterdam: Balkema; 2001. p. 49–97.
- [5] Palmström A. Measurements of and correlations between block size and Rock Quality Designation (RQD). *Tunnelling Undergr Sp Technol* 2005;20:362–77.
- [6] Wang LG, Yamashita S, Sugimoto F, Pan C, Tan G. A methodology for predicting the in situ size and shape distribution of rock blocks. *Rock Mech Rock Eng* 2003;36:121–42.
- [7] Sönmez H, Nefeslioglu HA, Gokceoglu C. Determination of wjd on rock exposures including wide spaced joints. *Rock Mech Rock Eng* 2004;37:403–13.
- [8] Kalenchuk KS, McKinnon S, Diederichs MS. Block geometry and rockmass characterization for prediction of dilution potential into sub-level cave mine voids. *Int J Rock Mech Min Sci* 2008;45:929–40.
- [9] Latham JP, Meulen JV, Dupray S. Prediction of in-situ block size distributions with reference to armourstone for breakwaters. *Eng Geol* 2006;86:18–36.
- [10] Yavuz AB, Turk N, Koca MY. Geological parameters affecting the marble production in the quarries along the southern flank of the Menderes Massif, in SW Turkey. *Eng Geol* 2005;80:214–41.
- [11] Nikolayev D, Siegesmund S, Mosch S, Hoffmann A. Model-based prediction of unfractured rock masses. *Z Dtsch Ges Geowissenschaften* 2007;158:483–90.
- [12] Prissang R, Hella P, Lehtimäki T, Saksa P, Nummela J, Vuento A. Localisation of undisturbed blocks in larger dimension stone rock masses. *Z Dtsch Ges Geowissenschaften* 2007;158:471–82.
- [13] Sousa LMO. Granite fracture index to check suitability of granite outcrops for quarrying. *Eng Geol* 2007;92:146–59.
- [14] Carvalho JF, Henriques P, Fale P, Luis G. Decision criteria for the exploration of ornamental-stone deposits: application to the marbles of the Portuguese Estremoz Anticline. *Int J Rock Mech Min Sci* 2008;45:1306–19.
- [15] Sousa LMO. Evaluation of joints in granitic outcrops for dimension stone exploitation. *J Eng Geol Hydrogeol* 2010;43:85–94.
- [16] Slob S, Hack H, Turner AK. An approach to automate discontinuity measurements of rock faces using laser scanning techniques. In: *Proceedings of EUROCK conference, Funchal, Portugal*; 25–28 November 2002. p. 87–94.
- [17] Siefko S, Hack R, van Knapen B, Turner K, Kemeny J. Method for automated discontinuity analysis of rock slopes with three-dimensional laser scanning. *Transp Res Rec* 2005;1913:187–94.
- [18] Mikos M, Vidmar A, Brilly M. Using a laser measurement system for monitoring morphological changes on the Strug rock fall, Slovenia. *Nat Hazards Earth Syst Sci* 2005;5:143–53.
- [19] Lim M, Petley DN, Rosser NJ, Allison RJ, Long AJ, Pybus D. Combined digital photogrammetry and time-of-flight laser scanning for monitoring cliff evolution. *Photogrammetry Rec* 2005;20:109–29.
- [20] Kemeny J, Norton B, Turner K. Rock slope stability analysis utilizing ground-based LIDAR and digital image processing. *Felsbau* 2006;24:8–15.
- [21] Kemeny J, Turner K, Norton B. LIDAR for Rock Mass Characterization: hardware, software, accuracy, and best practices. In: *Laser and photogrammetric methods for rock face characterization workshop, Golden Colorado*; 17–18 June, 2006. p. 49–62.
- [22] Strouth A, Eberhard E. The use of LIDAR to overcome rock slope hazard data collection challenges at Afternoon Creek, Washington. In: *Laser and photogrammetric methods for rock face characterization workshop, Golden Colorado*; 17–18 June, 2006. p. 71–82.
- [23] Sagy A, Brodsky EE, Axen GJ. Evolution of fault-surface roughness with slip. *Geology* 2007;35:283–6.
- [24] Enge HD, Buckley SJ, Rotevatn A, Howell JA. From outcrop to reservoir simulation model: workflow and procedures. *Geosphere* 2007;3:469–90.
- [25] Labourdette R, Jones RR. Characterization of fluvial architectural element using a three-dimensional outcrop data set: Escanilla braided system, South-Central Pyrenees, Spain. *Geosphere* 2007;3:422–34.
- [26] Otoo JN, Maerz NH, Xiaoling L, Duan Y. 3-D discontinuity orientations using combined optical imaging and LiDAR techniques. In: *Proceedings of the 45th US rock mechanics symposium, San Francisco*; 26–29 June, 2011. p. 9–14.

- [27] Mah J, Samson C, McKinnon SD. 3D laser imaging for joint orientation analysis. *Int J Rock Mech Min Sci* 2011;48:932–41.
- [28] Maerz NH, Otoo J, Kassebaum T, Boyko K Using LIDAR in highway rock cuts. In: Proceedings of the 63rd annual highway geology symposium, Redding, CA; 7–10 May, 2012. p. 13–17.
- [29] Post RM, Kemeny JM, Murphy R Image processing for automatic extraction of rock joint orientation data from digital images. In: Proceedings of the 38th U.S. rock mechanics symposium, Washington, D.C.; 7–10 July, 2001. p. 877–884.
- [30] Handy J, Kemeny J, Donovan J, Thiam S Automatic discontinuity characterization of rock faces using 3D laser scanners and digital imaging. In: Proceedings of the 41st US rock mechanics symposium, Houston; 5–10 June, 2004. p. 5–11.
- [31] Otoo JN, Maerz NH, Li X, Duan Y Verification of a 3-D LiDAR point cloud viewer for measuring discontinuity orientations. In: Proceedings of the 46th US Rock mechanics Symposium, Chicago; 24–27 June, 2012. p. 9–14.
- [32] Duan Y, Li X, Maerz NH, Otoo J Automatic 3D facet orientations estimation from LiDAR imaging. In: Proceedings of the NSF engineering research and innovation conference, Atlanta, Georgia; 4–7 January, 2011. p. 19–24.
- [33] Maerz NH, Youssef AM, Otoo JN, Kassebaum TJ, Duan Y. A simple method for measuring discontinuity orientations from terrestrial LIDAR images. *Env Eng Geosci* 2013;19:185–94.
- [34] Otoo JN. *Traces, Facets, and 3-D discontinuity orientation from combined LiDAR and optical imaging*. PhD Thesis. Rolla: Missouri University of Science and Technology; 2012.